

REVIEW ARTICLE

Non-linear Dynamics and Primordial Curvature Perturbations from Preheating

Andrei V. Frolov

Department of Physics, Simon Fraser University
8888 University Drive, Burnaby, BC Canada V5A 1S6
E-mail: frolov@sfu.ca

Abstract. In this paper I review the theory and numerical simulations of non-linear dynamics of preheating, a stage of dynamical instability at the end of inflation during which the homogeneous inflaton explosively decays and deposits its energy into excitation of other matter fields. I focus on preheating in chaotic inflation models, which proceeds via broad parametric resonance. I describe a simple method to evaluate Floquet exponents, calculating stability diagrams of Mathieu and Lame equations describing development of instability in $m^2\phi^2$ and $\lambda\phi^4$ preheating models. I discuss basic numerical methods and issues, and present simulation results highlighting non-equilibrium transitions, topological defect formation, late-time universality, turbulent scaling and approach to thermalization. I explain how preheating can generate large-scale primordial (non-Gaussian) curvature fluctuations manifest in cosmic microwave background anisotropy and large scale structure, and discuss potentially observable signatures of preheating.

Dedicated to the memory of Lev Kofman, a friend and a mentor, without whom this article would never have been written.

PACS numbers: 98.80.Cq, 05.10.-a

Submitted to: *Class. Quantum Grav. (special cluster issue)*

1. Introduction

The idea of inflation (a period of rapid quasi-exponential expansion of the Universe) neatly solves several long-standing issues in cosmology [1, 2], and has been spectacularly confirmed by observations of the Cosmic Microwave Background (CMB) anisotropies [3, 4]. While the Universe is inflating, its contents is cold. But eventually, inflation has to end and the field driving the inflation must decay, depositing energy into high-energy particles. This process, known as reheating, “boils” the vacuum and starts the thermal history of the universe with the hot big bang. As universe continues to cool down, it could undergo more phase transitions, which would happen at symmetry breaking points of the theory. Very little is known about the fundamental physics at these energy scales, and cosmological observations could be our only source of information for the foreseeable future. No photons reach us directly from this epoch as the universe is filled with hot plasma and is opaque until recombination. Nevertheless, the expansion history of the early universe is imprinted on the sky in the form of primordial curvature fluctuations. With success of WMAP and the data from Planck soon to come, CMB observations are reaching precision required to disentangle other subdominant effects from Gaussian fluctuations due to simple inflation [5].

The most basic models of reheating involve inflaton decaying into one or more other scalar fields. Among the most interesting are the ones where decay is non-perturbative, for example proceeding through parametric resonance naturally happening in chaotic inflation models [6, 7, 8, 9, 10, 11, 12], or tachyonic instability in hybrid inflation models [13, 14, 15]. For all their simplicity, these models have surprisingly rich physics involving non-equilibrium phase transitions. While initial stages of preheating are linear and instability development can be understood analytically [11, 12], dynamics could be chaotic [16], and the field evolution quickly becomes inhomogeneous and non-linear, so non-perturbative decay of the inflaton has to be studied numerically [17, 18, 19, 20, 21, 22, 23, 24, 25, 26, 27]. In this paper I briefly review the theory of parametric resonance, go over general results of numerical simulations of non-linear field evolution during preheating, and discuss signatures of preheating that could potentially be observed.

2. Analytical Theory of Preheating

The basic model of reheating involves inflaton ϕ decaying into another scalar field χ . The action describing two interacting scalar fields minimally coupled to gravity is

$$S = \int \left\{ \frac{R}{16\pi G} - \frac{1}{2} g^{\mu\nu} (\phi_{,\mu}\phi_{,\nu} + \chi_{,\mu}\chi_{,\nu}) - V(\phi, \chi) \right\} \sqrt{-g} d^4x, \quad (1)$$

with potential $V(\phi, \chi)$ containing the terms responsible for field masses and self-couplings, as well as their interaction. Polynomial field operators up to fourth order are renormalizable, so one usually takes $\frac{1}{2}m^2\phi^2$ or $\frac{1}{4}\lambda\phi^4$ inflaton potential for chaotic inflation, and $\frac{1}{2}g^2\phi^2\chi^2$ coupling term [11, 12]. For simplicity, one can keep the decay field χ massless. Couplings like $\frac{1}{2}\sigma\phi\chi^2$ are also allowed and could be present [26], although one would need a χ^4 self-interaction to keep the potential bounded from below. Models with various combinations of these potential bits have been studied in the literature; in this review, I will mainly focus on the one with quartic potential [12]

$$V(\phi, \chi) = \frac{1}{4}\lambda\phi^4 + \frac{1}{2}g^2\phi^2\chi^2. \quad (2)$$

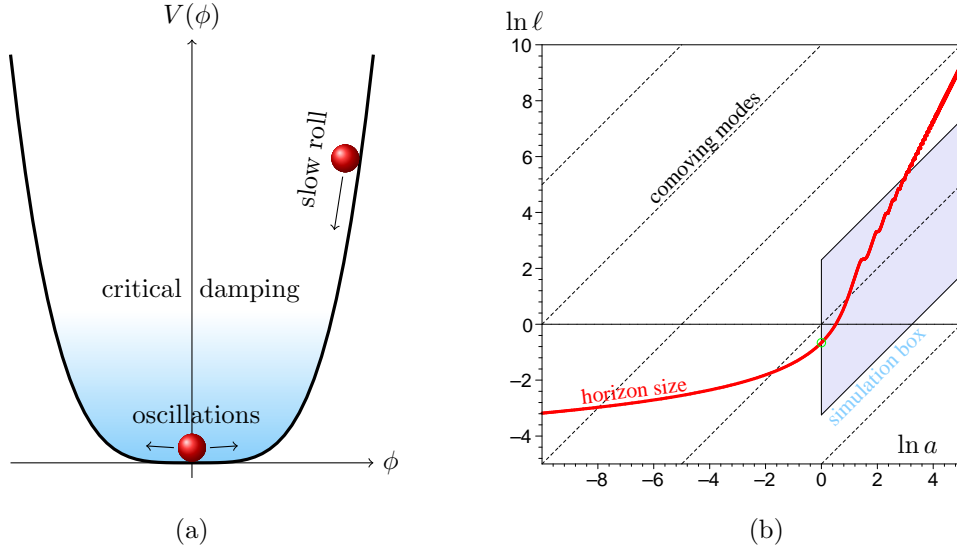


Figure 1. Dynamics of a single field chaotic inflation model with $\lambda\phi^4/4$ potential.

In a flat homogeneous isotropic universe with Friedmann-Robertson-Walker metric

$$ds^2 = -dt^2 + a(t)^2 d\mathbf{x}^2, \quad (3)$$

the field equations of motion are readily obtained from the action (1); they are

$$\ddot{\phi} + 3H\dot{\phi} + \left(-\frac{\Delta}{a^2} + \lambda\phi^2 + g^2\chi^2\right)\phi = 0, \quad (4)$$

$$\ddot{\chi} + 3H\dot{\chi} + \left(-\frac{\Delta}{a^2} + g^2\phi^2\right)\chi = 0. \quad (5)$$

Hubble parameter $H \equiv \dot{a}/a$ plays the role of friction term in field dynamics. Its value is determined by the (average) total energy density according to Friedmann equation

$$H^2 = \frac{8\pi G}{3}\langle\rho\rangle, \quad (6)$$

where the combined energy density of the two fields is

$$\rho = \frac{1}{2}\dot{\phi}^2 + \frac{1}{2}\dot{\chi}^2 + \frac{1}{2}\frac{(\nabla\phi)^2}{a^2} + \frac{1}{2}\frac{(\nabla\chi)^2}{a^2} + V(\phi, \chi). \quad (7)$$

During chaotic inflation, potential energy of the inflaton causes Hubble friction to be large, and the motion of the fields is over-damped. The inflaton ϕ slowly rolls down the potential until the damping becomes sub-critical, at which point it starts oscillating near the minimum of the potential with decreasing amplitude, as illustrated in Figure 1a. Evolution of the Hubble horizon size $L \equiv 1/H$ and the physical wavelength of comoving modes $\lambda \equiv 2\pi a/k$ is shown on Figure 1b. During inflation L changes slowly, so that slow roll parameter $\epsilon \equiv \frac{\partial \ln L}{\partial \ln a} \ll 1$. When field is oscillating, Hubble horizon size grows as $L \propto a^2$ according to the average equation of state, which is 1/3 for $\lambda\phi^4$ oscillator. Comoving modes stop exiting and begin re-entering the horizon when $\epsilon = 1$; this moment can be taken as the end of inflation.

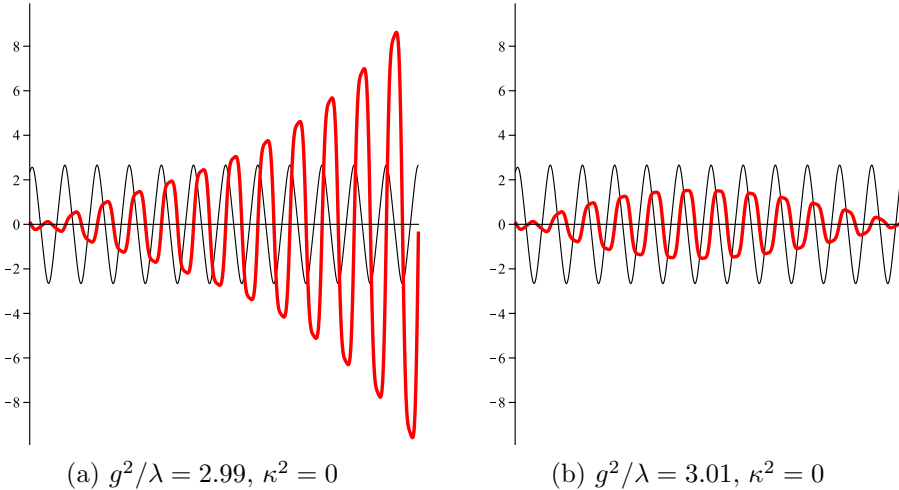


Figure 2. Background oscillations of the inflaton $a\phi$ (black) and the zero mode of decay field $a\chi$ (red) for values of coupling slightly inside (a) and outside (b) of the first resonance band in Figure 3b. Amplitude of $a\chi$ was scaled up by $3 \cdot 10^8$.

Other fields coupled to inflaton feel its oscillations through modulation of parameters in their equations of motion, such as the effective mass term $g^2\phi^2$ in equation (5). Periodic modulation can lead to parametric resonance and exponential growth of inhomogeneous excitations in the fields coupled to inflaton. This is a fairly generic feature of chaotic inflation models; let's see how this happens in our model (2).

It is very useful to scale variables so that the inflaton oscillations are periodic and of constant amplitude. This is particularly easy in model (2), which is conformally invariant apart from its coupling to gravity. Switching to conformal time $d\eta \equiv dt/a$ and scaling the field values according to their conformal weight, equation of motion for homogeneous inflaton (4) becomes simply $(a\phi)'' + \lambda(a\phi)^3 - a''\phi = 0$. If one neglects the last term (which is small as $a \simeq \eta$), oscillating inflaton solution is

$$\phi(\eta) = \frac{\Phi_0}{a(\eta)} f(\tau), \quad \tau \equiv \lambda^{\frac{1}{2}} \Phi_0 (\eta - \eta_0) \quad (8)$$

where Φ_0 is the amplitude of inflaton oscillations, and $f(\tau)$ is a unit amplitude solution of the canonical anharmonic oscillator equation $d^2 f / d\tau^2 + f^3 = 0$, which can be written exactly in terms of Jacobi elliptical cosine function, or its harmonic expansion [29]

$$f(\tau) \equiv \operatorname{cn}(\tau, 2^{-\frac{1}{2}}) = 2^{\frac{1}{2}} \frac{4\pi}{T} \sum_{n=1}^{\infty} \frac{\cos(n - \frac{1}{2}) \frac{4\pi}{T} \tau}{\cosh(n - \frac{1}{2}) \pi}. \quad (9)$$

Function $f(\tau)$ is periodic with period $T = \pi^{-\frac{1}{2}}\Gamma^2(\frac{1}{4})$, and its harmonic expansion is exponentially converging, so only a few terms are needed to accurately represent its shape. Substituting background inflaton solution (8) into equation of motion (5) for the coupled field χ , and rescaling variables the same way we did for inflaton, one obtains the evolution equation for the Fourier mode of decay field χ_k with comoving wavenumber k . In terms of rescaled parameters $\kappa \equiv k/(\lambda^{\frac{1}{2}}\Phi_0)$ and $q \equiv g^2/\lambda$, it is

$$\frac{d^2(a\chi_k)}{d\tau^2} + \left[\kappa^2 + q \operatorname{cn}^2(\tau, 2^{-1/2}) \right] (a\chi_k) = 0. \quad (10)$$

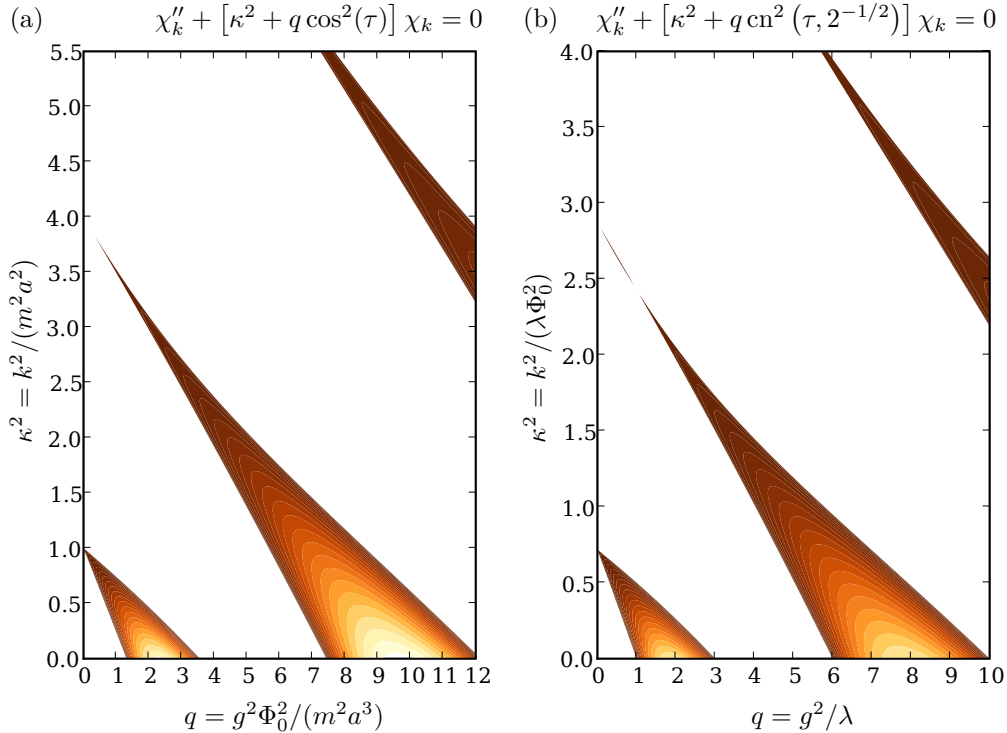


Figure 3. Stability diagram of Mathieu (a) and Lame (b) equations, using the same parametrization. White regions correspond to stable solutions, shaded regions are unstable, with brighter color corresponding to larger values of critical exponent μ (isolevels are spaced every $\Delta\mu = 0.01185$).

Exact solution of the oscillating inflaton $a\phi$ is shown in Figure 2, along with homogeneous solution of the field $a\chi$ coupled to it, for two slightly different values of the coupling g^2/λ . As you can see, depending on the value of the coupling, evolution of the field χ can be either exponentially unstable (2a), or merely oscillatory (2b).

Differential equations with periodic coefficients are studied in Floquet theory, and are often encountered in other branches of physics as well (for example, Bloch waves in condensed matter). Equation (10), in particular, is known as Lame equation, while its counterpart for harmonic inflaton oscillations in $m^2\phi^2$ potential is Mathieu equation [30]. According to Floquet's theorem, equation (10) admits solution of the form $e^{\mu\tau}P(\tau)$, where μ is a complex number, and function $P(\tau)$ is periodic. Floquet exponent μ depends on the parameters κ^2 and q , and can be calculated by explicitly constructing such periodic function from the principal fundamental matrix solution

$$\mathbb{W}(\tau) = \begin{bmatrix} \chi_1(\tau) & \chi_2(\tau) \\ \chi'_1(\tau) & \chi'_2(\tau) \end{bmatrix}, \quad (11)$$

made up from two independent solutions χ_1 and χ_2 with initial conditions $\mathbb{W}(0) = \mathbb{I}$. Integrating principal fundamental solution over a single period (which can be done efficiently and precisely using numerical integration), and fixing coefficients in a linear combination $c_1\chi_1(\tau) + c_2\chi_2(\tau) = e^{\mu\tau}P(\tau)$ to satisfy $P(T) = P(0)$ and $P'(T) = P'(0)$,

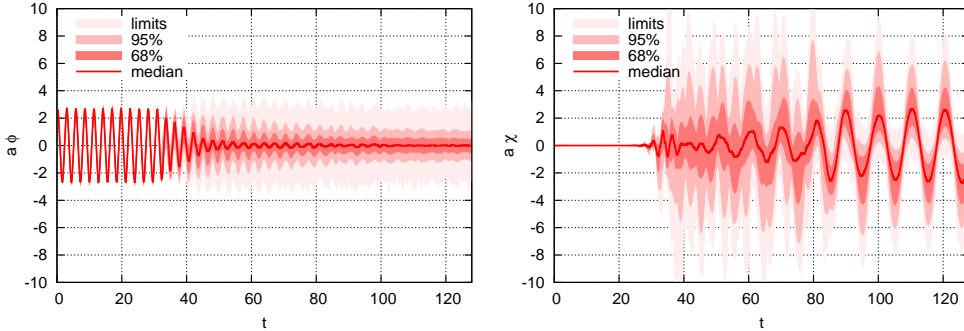


Figure 4. Evolution of distributions of inflaton (left) and decay product (right) in a full non-linear simulation with coupling at the maximal resonance $g^2/\lambda = 1.875$.

one finds that the value of Floquet exponent μ is given by

$$e^{\mu T} = Q(T) + \sqrt{Q^2(T) - W(T)}, \quad (12)$$

where Q and W are two invariants of the matrix \mathbb{W} under a similarity transformation

$$Q = \frac{1}{2} \text{tr } \mathbb{W}, \quad W = \det \mathbb{W} \equiv 1. \quad (13)$$

The second invariant (Wronskian W) is conserved, so expression (12) simplifies to

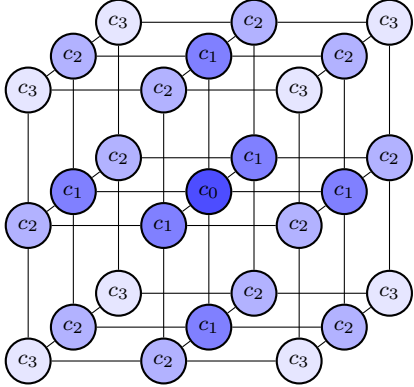
$$\cosh \mu T = Q(T). \quad (14)$$

Stability diagrams of Mathieu and Lame equations showing contour plots of $\text{Re}\mu$ calculated in this fashion are presented on Figure 3. Wide bands in parameter space are unstable, with values of Floquet exponent μ reaching as high as 0.237 for Lame equation. If the value of coupling lands you into one of these bands, inflaton will decay very efficiently into χ_k particles for a wide range of wavenumbers k . This regime is known as a broad parametric resonance.

Although not usually emphasized, the instability band structure of Lame and Mathieu equations is quite similar, as elliptic cosine (9) differs from $\cos \tau$ by 4.3% total harmonic distortion and 18% larger period. The real difference between $m^2\phi^2$ and $\lambda\phi^4$ models is how parameters scale with expansion of the universe. While their values stay constant for $\lambda\phi^4$ model (which is nearly conformally invariant), for $m^2\phi^2$ model expansion drags the values of parameters toward the stable point $\kappa^2 = q = 0$, eventually shutting off the resonance. Thus for preheating to be efficient in $m^2\phi^2$ model, one needs a much larger initial value of q .

3. Tackling Non-linear Evolution: Numerical Methods and Issues

Broad parametric resonance amplifies quantum fluctuations of the fields, creating real particles in a state far from thermal equilibrium. Instability is exponentially rapid, and develops within a few dozen of inflaton oscillation (as illustrated in Figure 4), which is very fast on cosmological time scales. Once the energy density of created particles becomes comparable to that of the homogeneous inflaton, one can no longer treat the evolution perturbatively, and non-linearity of the coupling and back reaction of the created particles on the inflaton evolution has to be taken into account. The



\$c_3\$	\$c_2\$	\$c_1\$	\$-c_0\$	cost	stability
(8)	(12)	(6)	(1)	$(\times, +)$	$\frac{\Delta t}{\Delta x} < \dots$
0	0	1	6	1, 6	$1/\sqrt{3}$
0	$\frac{1}{6}$	$\frac{1}{3}$	4	3, 18	$1/\sqrt{2}$
$\frac{1}{12}$	0	$\frac{2}{3}$	$\frac{14}{3}$	3, 14	$3/\sqrt{21}$
$\frac{1}{30}$	$\frac{1}{10}$	$\frac{7}{15}$	$\frac{64}{15}$	4, 26	$\sqrt{30}/8$

Figure 5. Three-dimensional spatial discretization stencil (left) and summary of coefficients (right) for minimal (top) and three isotropic discretization schemes.

most straightforward way to do it is to solve field evolution equations numerically [17, 18].

Several codes are available for this purpose, most notably LATTICEEASY by Gary Felder and Igor Tkachev [31, 32] which is widely used and modified, my own DEFROST [33] which offers improved performance and visualization capabilities, and a new GPU-accelerated CUDAEEASY by Jani Sainio [34]. A pseudo-spectral code PSpectRE has just been released as well [35]. Most of the implementations (with the exception of PSpectRE) opt for a finite difference method to solve non-linear partial differential equations (4,5). The fields are discretized on a cubic spatial grid of spacing dx , and the spatial differential operators are approximated by finite differences

$$\Delta X = \frac{D[X]}{(dx)^2}, \quad (\nabla X)^2 = \frac{G[X]}{(dx)^2}. \quad (15)$$

Discretizations of Laplacian operator involving only 26 nearest neighbours of a point

$$D[X] \equiv \underbrace{\sum_{x-1}^{x+1} \sum_{y-1}^{y+1} \sum_{z-1}^{z+1}}_{\alpha} c_{d(\alpha)} X_{\alpha} \quad (16)$$

is going to be second order accurate, but truncation error can be made isotropic to fourth order [36] by taking coefficients c_{α} as summarized in Figure 5. A critical issue for accuracy of long-term cosmological simulations is discretization of gradient terms in energy density (7). Discretized energy is not necessarily conserved by discretized equations of motion, and gradient energy leaking off the grid affects equation of state and leads to large cumulative errors in expansion history of the universe [47, 49]. The best way to avoid this pitfall is to discretize Lagrangian (1) directly. One can show that the proper discretization of gradient square, variation of which leads to Laplacian discretization (16) in equations of motion, is

$$G[X] \equiv \frac{1}{2} \underbrace{\sum_{x-1}^{x+1} \sum_{y-1}^{y+1} \sum_{z-1}^{z+1}}_{\alpha} c_{d(\alpha)} (X_{\alpha} - X_0)^2. \quad (17)$$

Once the spatial operators are discretized, time evolution problem becomes a system of coupled ordinary differential equations, which can be integrated using any of the

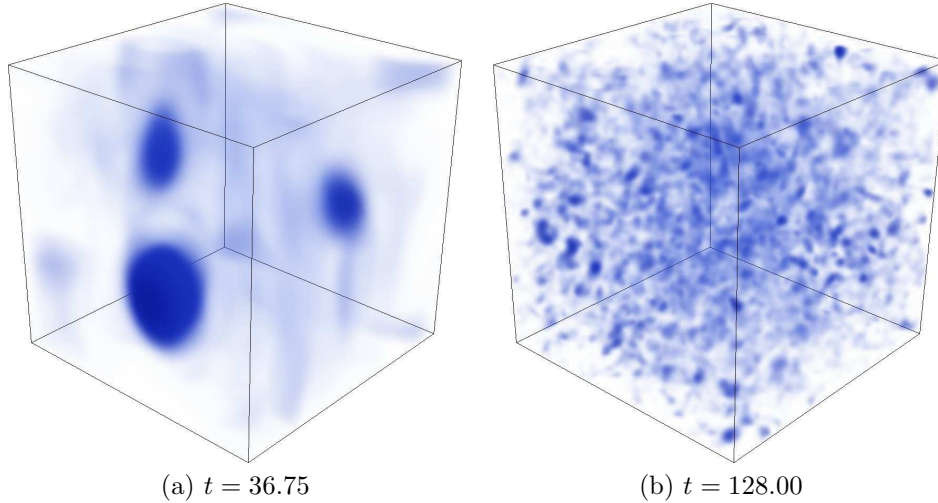


Figure 6. Energy density ρ inside the simulation box soon after onset of instability (a) and during subsequent evolution (b) in preheating model (2).

usual methods. DEFROST uses leapfrog scheme, which is simple, fast, and second order accurate in time. Higher order scheme could be used if needed. Symplectic integrator developed in [49] is capable of reaching machine precision levels, or hybrid integrator of Huang *et. al.* [28] could be used if time operator splitting is not possible.

4. Non-Linear Dynamics, Thermalization and Universality within Horizon

Non-linear dynamics that soon takes over the evolution of scalar fields can be rather non-trivial. Preheating is essentially a non-equilibrium phase transition, and a lot of interesting things can happen. Over the years, detailed numerical studies have been carried out for many parametric resonance [17, 18, 20, 25, 26, 27] and tachyonic [21, 22, 23, 24] preheating models. In this section, I highlight some features of non-linear dynamics in preheating on horizon scales. This is local physics as far as cosmology is concerned, as the Hubble horizon size at the end of chaotic inflation is tiny (roughly 1m redshifted to the present day).

Quantum fluctuations that fall into unstable bands of Figure 3 are amplified and become classical with large occupation numbers. Once linear instability develops, the field configuration becomes very inhomogeneous and particle description gets complicated by non-linear coupling. A useful tracer of field dynamics is the evolution of the total energy density (7), which is an adiabatic invariant for rapidly oscillating fields. Evolution of energy density ρ in preheating model (2) with $g^2/\lambda = 1.875$ is shown in Figure 6. For that value of the coupling, long wavelength fluctuations grow fastest, leading to formation of large blobs as shown in Figure 6a. Once density contrast increases to about one, non-linear interaction kicks in and the density fragments to much smaller scales as shown in Figure 6b. In particle description, this could be viewed as upscattering of modes to higher momenta by non-linear interaction term.

Just as it happens in phase transitions, one can also produce topological defects during preheating, if the theory allows them. For example, in preheating model with

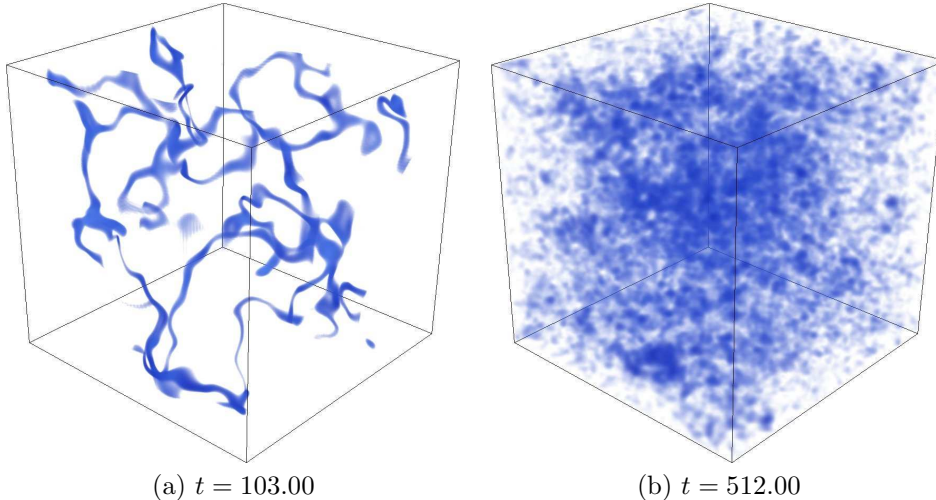


Figure 7. Transient formation of topological defects (a) and late-time energy density configuration (b) in preheating model (18) with global $O(2)$ symmetry.

$O(2)$ -symmetric potential with a small field vacuum expectation value v

$$V(\phi, \chi) = \frac{1}{4} \lambda (\phi^2 + \chi^2 - v^2)^2, \quad (18)$$

global cosmic strings can form [19, 20]. Initial instability in this model develops similarly to (2) with $g^2/\lambda = 2$, but once the energy density dilutes enough to fill the ring at the bottom of potential, cosmic strings are produced. String cores ($\phi^2 + \chi^2 < v^2/40$) soon after formation are shown in Figure 7a. String loops within horizon are transient, and eventually will collapse and annihilate. After a while, energy density configuration once again reaches a highly fragmented state shown in Figure 7b.

An important open question is exactly how and when thermalization after preheating happens. Characteristic momentum of particles produced during linear stage of preheating is determined by the instability band structure. Typically, it is significantly less than that of thermal equilibrium value, so particles need to upscatter through non-linear interactions, and thermalization can be delayed by a long time [11]. This is supported by numerical simulations, which show slow scaling regime in evolution of field occupation numbers in $\lambda\phi^4$ model [37, 38].

While dynamics of the non-equilibrium phase transition can be rather varied, late stages of preheating appear to have a certain universality to them. After initial transient, the field evolution leads to a highly inhomogeneous state similar to that shown in Figures 6b and 7b which persists on long time scales, with slow fragmentation going on. A striking feature of this regime is that one-point probability distribution function of energy density contrast $\delta \equiv \rho/\bar{\rho}$ appears to be statistically stationary, and universal across a class of preheating models [33]. Figure 8 shows late-time energy density PDFs (with dilution due to expansion scaled out) for four different preheating models ending via broad parametric resonance. All of them fit lognormal distribution

$$P(\rho) d\rho = \frac{1}{\sqrt{2\pi}\sigma} \exp\left[-\frac{(\ln \rho - \mu)^2}{2\sigma^2}\right] \frac{d\rho}{\rho}. \quad (19)$$

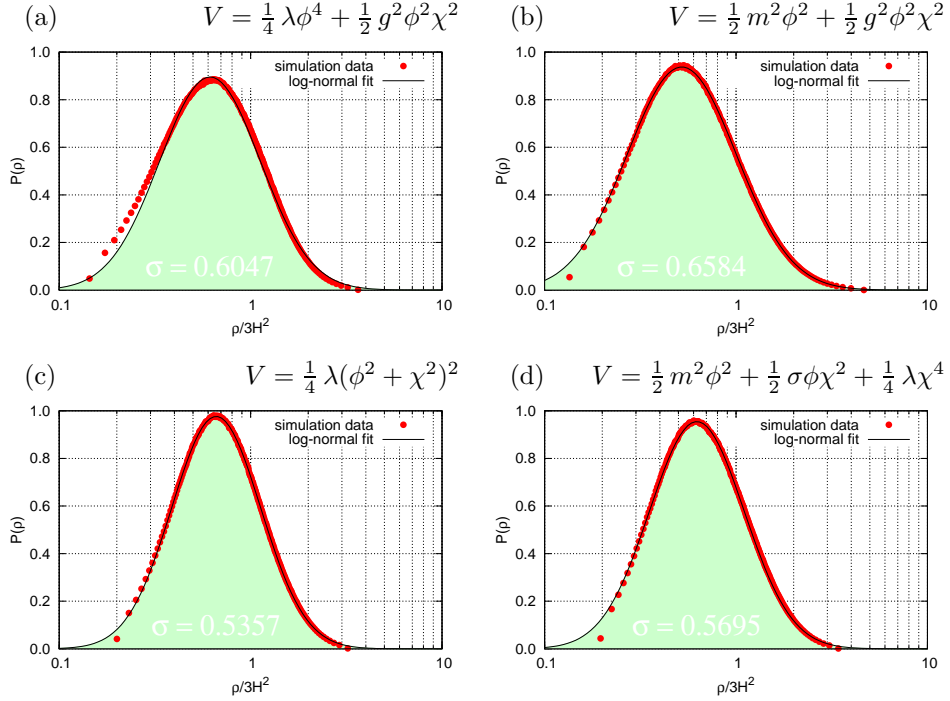


Figure 8. Universality of lognormal density distribution in various two-field preheating models with inflaton decaying via broad parametric resonance.

It is very tempting to attribute scaling and universality of the late stages of preheating to scalar field turbulence [37, 38], especially since lognormal density distributions are known to arise in relativistic fluid turbulence [39], but the subject needs further investigation.

5. Large-Scale Primordial Fluctuations from Preheating

As interesting as non-equilibrium field evolution could be, thermalization wipes out most of the details in the final state after the phase transition. However, dynamics of the transition could affect the expansion history of the universe, and leave an imprint in the observable large-scale curvature fluctuations produced during preheating [47, 49].

Inflation transforms sub-horizon quantum vacuum fluctuations in all the light fields into super-horizon classical fluctuations. These fluctuations are statistically homogeneous and isotropic Gaussian random fields, and are completely described by their spectra with amplitude $P(k) \sim H^2/4\pi^2$ evaluated at horizon crossing $H = k/a$. Causally disconnected patches on super-horizon scales evolve essentially independently, and large-scale curvature fluctuations Φ are the difference δN in amount of expansion $N \equiv \ln a$ different patches experience from the constant curvature hypersurface at the end of inflation to the constant density (and temperature) hypersurface once thermalization occurred [40, 41, 42]. Fluctuations of the inflaton $\delta\phi$ are usually the main source of metric curvature fluctuations Φ , with their amplitude enhanced by the slow-roll parameter $P_\Phi(k) = P_\phi(k)/(2m_{\text{pl}}^2\epsilon)$. It is also entirely

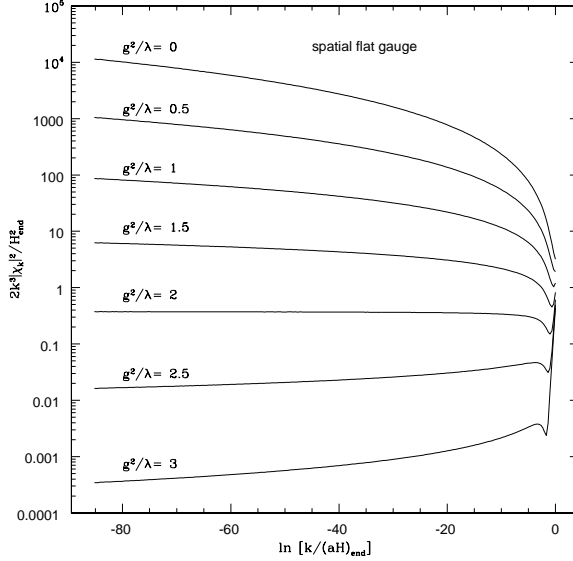


Figure 9. Primordial fluctuation spectrum of field χ produced by inflation [50].

possible to convert isocurvature modes from subdominant light fields into observable curvature perturbations, for example as it happens in curvaton-type scenarios [43, 44] and modulated reheating [45, 46]. Resonant preheating dynamics can create and significantly amplify curvature fluctuations from isocurvature modes of light fields, as suggested by [47, 48] and calculated in [49, 50].

For simple preheating model (2) with small values of coupling g^2/λ , the second field χ is light during inflation, and acquires fluctuation spectrum with power on super-horizon scales comparable to inflaton, as shown in Figure 9. Super-horizon fluctuations of χ are converted to curvature fluctuations through preheating dynamics. The basic mechanism is that the flat χ -direction of potential (2) is suddenly lifted due to expectation value of inhomogeneous terms like $\langle \delta\phi^2 \rangle$ when parametric resonance instability develops [49]. This will modulate equation of state based on the value of homogeneous mode in field χ at a time inhomogeneity develops, and create curvature fluctuations dependent on initial value of χ on super-horizon scales.

Calculating curvature fluctuations generated by preheating involves tracing minute differences in expansion history, from the end of inflation to thermalization, in non-linear three dimensional simulations of regions of the universe corresponding to different initial values of χ on super-horizon scales. This is a very demanding numerical problem, not only in terms of computing power, but precision required. The first attempt encountered numerical difficulties [47, 48], and it required development of new numerical integration techniques to obtain the answer [49]. Skipping a lot of technical details which will be discussed elsewhere [50], the total curvature fluctuation Φ produced in the inflation model (2) is

$$\Phi(\mathbf{x}) = \Phi_G(\mathbf{x}) + F_{\text{NL}}(\chi_G(\mathbf{x})), \quad (20)$$

where Φ_G is the usual nearly Gaussian contribution from inflaton fluctuations $\delta\phi$, and the second *uncorrelated* term is generated by preheating from the super-horizon

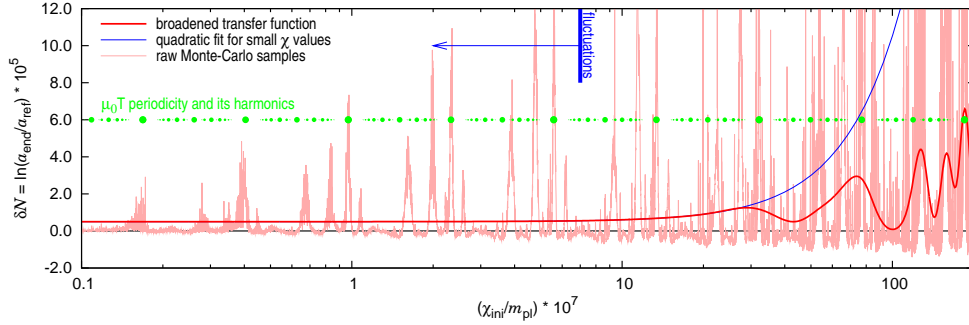


Figure 10. Non-linear transfer function $F_{\text{NL}}(\chi)$ connecting initial value of super-horizon mode χ_{ini} with curvature fluctuation δN it produces [49]. Thick red line shows result of averaging over substructure not resolved in CMB observations.

mode of the field χ . The exact distribution of the field χ sampled on observable part of the sky depends on inflation history in extreme version of cosmic variance. The transfer function F_{NL} shown in Figure 10 is quite non-linear and could lead to non-Gaussian fluctuations of the form very different from the usual weak non-Gaussianity parametrization

$$\Phi(\mathbf{x}) = \Phi_G(\mathbf{x}) + f_{\text{NL}}\Phi_G^2(\mathbf{x}). \quad (21)$$

The amplitude of curvature fluctuations produced by preheating in model (2) is 10^{-5} , which is comparable to the curvature fluctuations from inflaton, so the two could potentially be disentangled by searching for non-Gaussian component in the observed CMB temperature anisotropy.

6. Discussion: Going after Observable Signatures of Preheating

Very little is known about how inflation actually ended, and what was the high energy physics like at those energy scales (or even what is the inflaton itself). Traces of reheating are hidden from us by opaque plasma in nearly thermal state, and are unobservable directly. One must seek signatures of preheating that survive thermalization and could be detected. These could include stable relics like topological defects [19, 20, 53] or primordial black holes [54, 55, 56], stochastic gravitational wave background produced by inhomogeneities during reheating [57, 58, 59, 60, 61, 62], or anomalies in the expansion history of the universe imprinted in the primordial curvature fluctuations [45, 46, 47, 48, 49, 50, 51, 52]. Of these, the last effect appears to be the most promising observationally, as stable relic formation is difficult without spoiling cosmology, and stochastic gravitational waves are very hard to detect.

Curiously enough, the simple model of preheating (2) could generate non-Gaussian curvature fluctuations of observable amplitude which are intermittent, producing primordial “cold spots” [49]. Although arguable [4], the CMB temperature map appears to have slight statistical anomalies in the form of a cold spot in the southern hemisphere [63], and slight discrepancy in north-south temperature anisotropy spectra [64]. Exciting possibility is that primordial “cold spot”, whether from preheating or some other early universe source, could potentially explain both. A tell-tale signature of *primordial* non-Gaussian cold spot is the associated *E-mode*

polarization pattern around it, which might be possible to test with Planck data [65]. Primordial potential “dips” would also manifest in formation of large scale structure.

References

- [1] A. D. Linde, “*Particle physics and inflationary cosmology*,” Contemp. Concepts Phys. **5**, 1-362 (1990) [[arXiv:hep-th/0503203](#)].
- [2] A. Linde, “*Inflation and string cosmology*,” eConf **C040802**, L024 (2004) [J. Phys. Conf. Ser. **24**, 151 (2005 PTPSA,163,295-322.2006)] [[arXiv:hep-th/0503195](#)].
- [3] E. Komatsu *et al.*, “*Seven-Year Wilkinson Microwave Anisotropy Probe (WMAP) observations: Cosmological interpretation*,” [arXiv:1001.4538](#) [astro-ph.CO].
- [4] C. L. Bennett *et al.*, “*Seven-Year Wilkinson Microwave Anisotropy Probe (WMAP) observations: Are there cosmic microwave background anomalies?*,” [arXiv:1001.4758](#) [astro-ph.CO].
- [5] E. Komatsu *et al.*, “*Non-Gaussianity as a probe of the physics of the primordial universe and the astrophysics of the low redshift universe*,” [arXiv:0902.4759](#) [astro-ph.CO].
- [6] A. D. Dolgov and D. P. Kirilova, “*Production of particles by a variable scalar field*,” Sov. J. Nucl. Phys. **51**, 172 (1990) [Yad. Fiz. **51**, 273 (1990)].
- [7] J. H. Traschen and R. H. Brandenberger, “*Particle production during out-of-equilibrium phase transitions*,” Phys. Rev. D **42**, 2491 (1990).
- [8] L. Kofman, A. D. Linde and A. A. Starobinsky, “*Reheating after inflation*,” Phys. Rev. Lett. **73**, 3195 (1994) [[arXiv:hep-th/9405187](#)].
- [9] Y. Shtanov, J. H. Traschen and R. H. Brandenberger, “*Universe reheating after inflation*,” Phys. Rev. D **51**, 5438 (1995) [[arXiv:hep-ph/9407247](#)].
- [10] L. Kofman, A. D. Linde and A. A. Starobinsky, “*Non-thermal phase transitions after inflation*,” Phys. Rev. Lett. **76**, 1011 (1996) [[arXiv:hep-th/9510119](#)].
- [11] L. Kofman, A. D. Linde and A. A. Starobinsky, “*Towards the theory of reheating after inflation*,” Phys. Rev. D **56**, 3258 (1997) [[arXiv:hep-ph/9704452](#)].
- [12] P. B. Greene, L. Kofman, A. D. Linde and A. A. Starobinsky, “*Structure of resonance in preheating after inflation*,” Phys. Rev. D **56**, 6175 (1997) [[arXiv:hep-ph/9705347](#)].
- [13] A. D. Linde, “*Hybrid inflation*,” Phys. Rev. D **49**, 748 (1994) [[arXiv:astro-ph/9307002](#)].
- [14] J. Garcia-Bellido and A. D. Linde, “*Preheating in hybrid inflation*,” Phys. Rev. D **57**, 6075 (1998) [[arXiv:hep-ph/9711360](#)].
- [15] G. N. Felder, L. Kofman and A. D. Linde, “*Instant preheating*,” Phys. Rev. D **59**, 123523 (1999) [[arXiv:hep-ph/9812289](#)].
- [16] D. I. Podolsky and A. A. Starobinsky, “*Chaotic reheating*,” Grav. Cosmol. Suppl. **8N1**, 13 (2002) [[arXiv:astro-ph/0204327](#)].
- [17] S. Y. Khlebnikov and I. I. Tkachev, “*Classical decay of inflaton*,” Phys. Rev. Lett. **77**, 219 (1996) [[arXiv:hep-ph/9603378](#)].
- [18] T. Prokopec and T. G. Roos, “*Lattice study of classical inflaton decay*,” Phys. Rev. D **55**, 3768 (1997) [[arXiv:hep-ph/9610400](#)].
- [19] S. Kasuya and M. Kawasaki, “*Topological defects formation after inflation on lattice simulation*,” Phys. Rev. D **58**, 083516 (1998) [[arXiv:hep-ph/9804429](#)].
- [20] I. Tkachev, S. Khlebnikov, L. Kofman and A. D. Linde, “*Cosmic strings from preheating*,” Phys. Lett. B **440**, 262 (1998) [[arXiv:hep-ph/9805209](#)].
- [21] G. N. Felder, J. Garcia-Bellido, P. B. Greene, L. Kofman, A. D. Linde and I. Tkachev, “*Dynamics of symmetry breaking and tachyonic preheating*,” Phys. Rev. Lett. **87**, 011601 (2001) [[arXiv:hep-ph/0012142](#)].
- [22] G. N. Felder, L. Kofman and A. D. Linde, “*Tachyonic instability and dynamics of spontaneous symmetry breaking*,” Phys. Rev. D **64**, 123517 (2001) [[arXiv:hep-th/0106179](#)].
- [23] E. J. Copeland, S. Pascoli and A. Rajantie, “*Dynamics of tachyonic preheating after hybrid inflation*,” Phys. Rev. D **65**, 103517 (2002) [[arXiv:hep-ph/0202031](#)].
- [24] J. Garcia-Bellido, M. Garcia Perez and A. Gonzalez-Arroyo, “*Symmetry breaking and false vacuum decay after hybrid inflation*,” Phys. Rev. D **67**, 103501 (2003) [[arXiv:hep-ph/0208228](#)].
- [25] D. I. Podolsky, G. N. Felder, L. Kofman and M. Peloso, “*Equation of state and beginning of thermalization after preheating*,” Phys. Rev. D **73**, 023501 (2006) [[arXiv:hep-ph/0507096](#)].
- [26] J. F. Dufaux, G. N. Felder, L. Kofman, M. Peloso and D. Podolsky, “*Preheating with trilinear interactions: Tachyonic resonance*,” JCAP **0607**, 006 (2006) [[arXiv:hep-ph/0602144](#)].
- [27] G. N. Felder and L. Kofman, “*Nonlinear inflaton fragmentation after preheating*,” Phys. Rev. D **75**, 043518 (2007) [[arXiv:hep-ph/0606256](#)].

- [28] N. Barnaby, J. R. Bond, Z. Huang and L. Kofman, “*Preheating after modular inflation*,” JCAP **0912**, 021 (2009) [[arXiv:0909.0503 \[hep-th\]](#)].
- [29] A. Kiper, “Fourier series coefficients for powers of the Jacobian elliptic functions,” Mathematics of Computation **43**, 247-259 (1984).
- [30] H. Bateman, “*Higher transcendental functions (Volume III)*,” McGraw-Hill (1955).
- [31] G. N. Felder and I. Tkachev, “*LATTICEEASY: A program for lattice simulations of scalar fields in an expanding universe*,” [arXiv:hep-ph/0011159](#).
- [32] G. N. Felder, “*CLUSTEREASY: A program for simulating scalar field evolution on parallel computers*,” [arXiv:0712.0813 \[hep-ph\]](#).
- [33] A. V. Frolov, “*DEFROST: A new code for simulating preheating after inflation*,” JCAP **0811**, 009 (2008) [[arXiv:0809.4904 \[hep-ph\]](#)].
- [34] J. Sainio, “*CUDAEEASY - a GPU accelerated cosmological lattice program*,” [arXiv:0911.5692 \[astro-ph.IM\]](#).
- [35] R. Easter, H. Finkel and N. Roth, “*PSpectRe: A pseudo-spectral code for (p)reheating*,” [arXiv:1005.1921 \[astro-ph.CO\]](#).
- [36] M. Patra and M. Karttunen, “*Stencils with isotropic discretization error for differential operators*,” Num. Meth. for PDEs **22**, 936 (2005).
- [37] R. Micha and I. I. Tkachev, “*Relativistic turbulence: A long way from preheating to equilibrium*,” Phys. Rev. Lett. **90**, 121301 (2003) [[arXiv:hep-ph/0210202](#)].
- [38] R. Micha and I. I. Tkachev, “*Turbulent thermalization*,” Phys. Rev. D **70**, 043538 (2004) [[arXiv:hep-ph/0403101](#)].
- [39] A. Nordlund and P. Padoan, “*Density PDFs of super-sonic turbulence*,” [arXiv:astro-ph/9810074](#).
- [40] A. Starobinsky, “*Dynamics of phase transition in the new inflationary universe scenario and generation of perturbations*,” Phys. Lett. B **117** (1982) 175.
- [41] D. S. Salopek and J. R. Bond, “*Nonlinear evolution of long wavelength metric fluctuations in inflationary models*,” Phys. Rev. D **42**, 3936 (1990).
- [42] M. Sasaki and E. D. Stewart, “*A general analytic formula for the spectral index of the density perturbations produced during inflation*,” Prog. Theor. Phys. **95**, 71 (1996) [[arXiv:astro-ph/9507001](#)].
- [43] A. D. Linde and V. F. Mukhanov, “*Nongaussian isocurvature perturbations from inflation*,” Phys. Rev. D **56**, 535 (1997) [[arXiv:astro-ph/9610219](#)].
- [44] D. H. Lyth and D. Wands, “*Generating the curvature perturbation without an inflaton*,” Phys. Lett. B **524**, 5 (2002) [[arXiv:hep-ph/0110002](#)].
- [45] G. Dvali, A. Gruzinov and M. Zaldarriaga, “*A new mechanism for generating density perturbations from inflation*,” Phys. Rev. D **69**, 023505 (2004) [[arXiv:astro-ph/0303591](#)].
- [46] L. Kofman, “*Probing string theory with modulated cosmological fluctuations*,” [arXiv:astro-ph/0303614](#).
- [47] A. Chambers and A. Rajantie, “*Lattice calculation of non-Gaussianity from preheating*,” Phys. Rev. Lett. **100**, 041302 (2008) [Erratum-ibid. **101**, 149903 (2008)] [[arXiv:0710.4133 \[astro-ph\]](#)].
- [48] A. Chambers and A. Rajantie, “*Non-Gaussianity from massless preheating*,” JCAP **0808**, 002 (2008) [[arXiv:0805.4795 \[astro-ph\]](#)].
- [49] J. R. Bond, A. V. Frolov, Z. Huang and L. Kofman, “*Non-Gaussian spikes from chaotic billiards in inflation preheating*,” Phys. Rev. Lett. **103**, 071301 (2009) [[arXiv:0903.3407 \[astro-ph.CO\]](#)].
- [50] J. R. Bond, A. V. Frolov, Z. Huang and L. Kofman, in preparation.
- [51] K. Kohri, D. H. Lyth and C. A. Valenzuela-Toledo, “*On the generation of a non-gaussian curvature perturbation during preheating*,” JCAP **1002**, 023 (2010) [[arXiv:0904.0793 \[hep-ph\]](#)].
- [52] A. Chambers, S. Nurmi and A. Rajantie, “*Non-Gaussianity from resonant curvaton decay*,” JCAP **1001**, 012 (2010) [[arXiv:0909.4535 \[astro-ph.CO\]](#)].
- [53] R. A. Battye and J. Weller, “*Cosmic structure formation in hybrid inflation models*,” Phys. Rev. D **61**, 043501 (2000) [[arXiv:astro-ph/9810203](#)].
- [54] S. G. Rubin, M. Y. Khlopov and A. S. Sakharov, “*Primordial black holes from non-equilibrium second order phase transition*,” Grav. Cosmol. **S6**, 51 (2000) [[arXiv:hep-ph/0005271](#)].
- [55] T. Suyama, T. Tanaka, B. Bassett and H. Kudoh, “*Are black holes over-produced during preheating?*,” Phys. Rev. D **71**, 063507 (2005) [[arXiv:hep-ph/0410247](#)].
- [56] T. Suyama, T. Tanaka, B. Bassett and H. Kudoh, “*Black hole production in tachyonic preheating*,” JCAP **0604**, 001 (2006) [[arXiv:hep-ph/0601108](#)].
- [57] R. Easter and E. A. Lim, “*Stochastic gravitational wave production after inflation*,” JCAP

- 0604**, 010 (2006) [[arXiv:astro-ph/0601617](#)].
- [58] R. Easther, J. T. . Giblin and E. A. Lim, “*Gravitational wave production at the end of inflation,*” Phys. Rev. Lett. **99**, 221301 (2007) [[arXiv:astro-ph/0612294](#)].
- [59] J. Garcia-Bellido and D. G. Figueroa, “*A stochastic background of gravitational waves from hybrid preheating,*” Phys. Rev. Lett. **98**, 061302 (2007) [[arXiv:astro-ph/0701014](#)].
- [60] J. Garcia-Bellido, D. G. Figueroa and A. Sastre, “*A gravitational wave background from reheating after hybrid inflation,*” Phys. Rev. D **77**, 043517 (2008) [[arXiv:0707.0839](#) [hep-ph]].
- [61] J. F. Dufaux, A. Bergman, G. N. Felder, L. Kofman and J. P. Uzan, “*Theory and numerics of gravitational waves from preheating after inflation,*” Phys. Rev. D **76**, 123517 (2007) [[arXiv:0707.0875](#) [astro-ph]].
- [62] C. Caprini, R. Durrer and G. Servant, “*Gravitational wave generation from bubble collisions in first-order phase transitions: An analytic approach,*” [arXiv:0711.2593](#) [astro-ph].
- [63] M. Cruz, E. Martinez-Gonzalez and P. Vielva, “*The WMAP cold spot,*” [arXiv:0901.1986](#) [astro-ph].
- [64] H. K. Eriksen, A. J. Banday, K. M. Gorski, F. K. Hansen and P. B. Lilje, “*Hemispherical power asymmetry in the three-year Wilkinson Microwave Anisotropy Probe sky maps,*” Astrophys. J. **660**, L81 (2007) [[arXiv:astro-ph/0701089](#)].
- [65] P. Vielva, E. Martinez-Gonzalez, M. Cruz, R. B. Barreiro and M. Tucci, “*CMB polarization as a probe of the anomalous nature of the cold spot,*” [arXiv:1002.4029](#) [astro-ph.CO].